Signal Processing 12 (1987) 83-91
North-Holland

UNWARPING OF SLIGHTLY DISTORTED PERIODIC STRUCTURES USING BIDIMENSIONAL POLYNOMIAL REPRESENTATIONS

Michael UNSER (Member EURASIP) and Murray EDEN

Biomedical Engineering and Instrumentation Branch, Division of Research Services, National Institute of Health, Bethesda, MD 20892, U.S.A.

Benes L. TRUS

Computer Systems Laboratory, Division of Computer Research and Technology, National Institute of Health, Bethesda, MD 20892, U.S.A.

Received 12 June 1986

Abstract. This paper describes a method to compensate for spatial distortion in quasi-periodic structures allowing a noise reduction by averaging. The successive steps of processing are preprocessing by local normalization, the detection of control points by cross-correlation, the estimation and compensation of the warping function using bidimensional polynomials, and finally noise reduction by filtering or accumulation. This method is applied to the improvement of high resolution images of thin sections of muscle fibers obtained by electron microscopy.

Zusammenfassung. Dieser Beitrag beschreibt ein Verfahren, räumliche Verzerrungen in quasiperiodischen Strukturen zu kompensieren und überlagertes Rauschen mit Hilfe einer Mittelwertbildung zu reduzieren. Die aufeinanderfolgenden Verarbeitungsschritte sind: Vorverarbeitung durch lokale Normalisierung, Detektion von Orientierungspunkten mit Hilfe der Kreuzkorrelation, Abschätzung und Kompensation der Verzerrungsfunktion mit Hilfe zweidimensionaler Polynome, und schließlich die Reduktion des Rauschens durch Filterung oder Akkumulieren. Diese Methode wird dazu angewendet, die Qualität hochauflösender Bilder von dünnen Sektionen von Muskelfasern zu verbessern, die mit Hilfe eines Elektronenmikroskops gewonnen werden.

Résumé. Cet article décrit une méthode pour la compensation de déformations spatiales pour des structures quasi-périodiques en vue d'une réduction du bruit par cumulation. Le traitement comporte les étapes suivantes: le prétraitement par normalisation locale, la détection par corrélation de points de contrôle caractérisant la position des cellules de base, l'estimation et la compensation de la fonction de déformation par l'intermédiaire de polynômes bidimensionnels, et finalement la réduction du bruit par filtrage ou cumulation. Cette technique est appliquée à l'amélioration d'images de filaments musculaires obtenues par microscopie électronique à très haute résolution.

Keywords. Texture analysis, periodicity, unwarping, bidimensional polynomial, noise reduction, image restoration.

1. Introduction

Image averaging techniques are commonly used to improve signal-to-noise ratios and have proven to be particularly useful in the analysis of high resolution micrographs, particularly as applied to structural investigations of biological macromolecules [3, 6]. For truly periodic or crystalline structures, an important noise reduction is possible by filtering out the nonperiodic component [1, 7]. This procedure is either implemented in the Fourier domain by masking out the nonperiodic components of the spectrum, or in real space by summing up spatially aligned replications of the original unit cell.

However, natural repetitive structures or textures are often not truly periodic and should rather be considered as originating from an ideal periodic

0165-1684/87/$3.50 © 1987, Elsevier Science Publishers B. V. (North-Holland)

model which has been distorted geometrically [4]. The purpose of this paper is to describe a procedure that allows the correction of this defect and thus produces images that can easily be processed for noise reduction and enhancement. This technique uses two-dimensional polynomial representations that have been described in a previous paper [2].

The presentation is organized as follows. Section 2 describes a method that uses a set of control or reference points to estimate a spatial warping function based on bidimensional polynomials. The different steps of processing, which include preprocessing, the location of reference points, spatial unwarping and noise reduction, are considered in Section 3. Finally, in Section 4, the method is applied to the enhancement of high resolution electron micrographs of slightly distorted thin sections of muscle filaments.

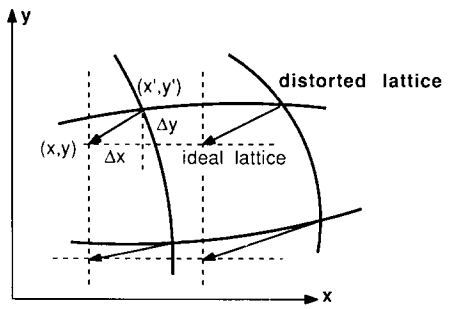

Fig. 1. Mapping of a geometrically distorted lattice into an ideal rectangular lattice.

2. Principle of bidimensional unwarping

2.1. Model of spatial distortion

The effect of spatial distortion may be represented by a one-to-one mapping between the spatial coordinates (x, y) of a gray level value in an ideal coordinate system and its corresponding (x', y') location in a distorted lattice. For convenience, this distortion may be decomposed into a horizontal and a vertical component as illustrated in Fig. 1. Accordingly, we define the relation between the (x, y) and (x', y') coordinate systems as

$$\begin{cases} x' = x + \Delta x(x, y), \\ y' = y + \Delta y(x, y). \end{cases} \tag{1}$$

A mathematically useful representation is obtained when the vertical and horizontal components of the distortion are expressed as bidimensional polynomial functions of the x- and y-coordinates:

$$\Delta x(x, y) = \sum_{i=1}^{M} \sum_{j=1}^{N} a_{i,j} x^{i-1} y^{j-1}, \tag{2}$$

$$\Delta y(x, y) = \sum_{i=1}^{M} \sum_{j=1}^{N} b_{i,j} x^{i-1} y^{j-1}. \tag{3}$$

The main advantage of a representation based on polynomial basis functions is that it is particularly well suited for simple geometrical transformations such as a rotation or projection of the coordinate system. For example, only four coefficient polynomials are required to map any skewed lattice into a perfect rectangular system. An increase of the order of the polynomials allows the modeling of virtually any geometrical transformation.

2.2. Estimation of the warping function

Let us consider a set of $K \times L$ control or reference points $\{(x'_{i,j}, y'_{i,j}),\ i = 1, 2, \ldots, K$ and $j = 1, 2, \ldots, L\}$ which we want to map, according to equations (1), (2), and (3), into a set of spatial coordinates $\{(x_{i,j}, y_{i,j}),\ i = 1, 2, \ldots, K,\ j = 1, 2, \ldots, L\}$ defined on an ideal nondistorted lattice. Using the separability property of bidimensional polynomials, which has been demonstrated in [6], it is possible to show that two uniquely defined polynomials allowing such a mapping exist, provided that the points on the undistorted lattice are chosen such that $\{(x_{i,j}, y_{i,j}) = (x_i, y_j),\ i = 1, 2, \ldots, K, j = 1, 2, \ldots, L\}$. Defining the $K \times L$ vertical and horizontal correction matrices as

$$\begin{cases} \Delta \boldsymbol{X} = [(x'_{i,j} - x_{i,j})], \\ \Delta \boldsymbol{Y} = [(y'_{i,j} - y_{i,j})], \end{cases} \tag{4}$$

the coefficients of these polynomials are computed

from

$$\boldsymbol{A} = [a_{i,j}] = \boldsymbol{V}_x^{-1}\,\Delta\boldsymbol{X}(\boldsymbol{V}_y^{-1})^{\mathrm{T}}, \tag{5}$$

$$\boldsymbol{B} = [b_{i,j}] = \boldsymbol{V}_x^{-1}\,\Delta\boldsymbol{Y}(\boldsymbol{V}_y^{-1})^{\mathrm{T}}, \tag{6}$$

where $\boldsymbol{V}_x = \boldsymbol{V}(x_1, x_2, \ldots, x_K)$ and $\boldsymbol{V}_y = \boldsymbol{V}(y_1, y_2, \ldots, y_L)$ are $K \times K$ and $L \times L$ Vandermonde matrices, respectively. A Vandermonde matrix, which we designate by $\boldsymbol{V}$, is a matrix of the form

$$\boldsymbol{V}(x_1, x_2, \ldots, x_K) = \begin{bmatrix} 1 & x_1^1 & \cdots & x_1^{K-1} \\ 1 & x_2^1 & \cdots & x_2^{K-1} \\ \vdots & \vdots & \cdots & \vdots \\ 1 & x_K^1 & \cdots & x_K^{K-1} \end{bmatrix}. \tag{7}$$

Note that equations (5) and (6) define one-to-one linear mappings between the correction matrices $\Delta\boldsymbol{X}$ and $\Delta\boldsymbol{Y}$, and the $K \times L$ polynomial coefficient matrices $\boldsymbol{A}$ and $\boldsymbol{B}$. A particularly efficient evaluation of polynomial coefficients is possible using the algorithm presented in [2], which allows a fast recursive inversion of Vandermonde matrices.

2.3. Unwarping

The principle of unwarping is as follows: First, a sampling grid is defined on the ideal undistorted lattice and is mapped, using (1), onto the observed image. The unwarped reconstructed image is finally obtained by interpolating the distorted picture and resampling it at those particular spatial coordinates. Using the estimated polynomial coefficients, which have been defined in the previous section, the vertical and horizontal correction factor at location (x, y) are obtained from

$$\begin{aligned} \Delta x(x, y) &= x' - x \\ &= [1 \;\; x^1 \;\; x^2 \;\; \cdots \;\; x^{K-1}] \\ &\quad \times \boldsymbol{A}[1 \;\; y^1 \;\; y^2 \;\; \cdots \;\; y^{L-1}]^{\mathrm{T}}, \\ \Delta y(x, y) &= y' - y \\ &= [1 \;\; x^1 \;\; x^2 \;\; \cdots \;\; x^{K-1}] \\ &\quad \times \boldsymbol{B}[1 \;\; y^1 \;\; y^2 \;\; \cdots \;\; y^{L-1}]^{\mathrm{T}}. \end{aligned} \tag{8}$$

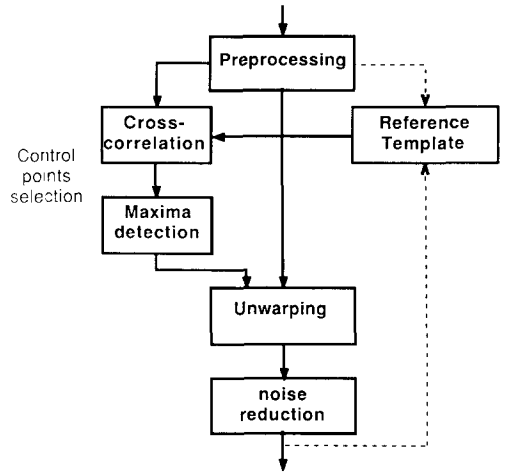

Fig. 2. Functional block diagram of a complete processing system.

3. General system description

The block diagram of an image processing system for the analysis of a slightly distorted pseudo-periodic structures is depicted in Fig. 2. The different steps of processing are described below.

3.1. Preprocessing

The preprocessing unit reduces sensitivity to external extraneous factors such as varying acquisition conditions or spatial data or transducer non-uniformities. We have used a local normalization algorithm which has been designed primarily for the treatment of homogeneous texture regions [10]. The preprocessed image is computed as

$$z_{k,l} = (t_{k,l} - m_{k,l})/s_{k,l}, \tag{9}$$

where $\{t_{k,l}\}$ denotes the input image, and where $\{m_{k,l}\}$ and $\{s_{k,l}\}$ are local estimates respectively of the mean and standard deviation computed over an $M' \times M'$ window which is centered on the current spatial location. The local correction factors are obtained by applying an $M' \times M'$ moving average filter to the input image and to the rectified high-pass filtered sequence $|t_{k,l} - m_{k,l}|$, respectively. The averaging window is usually chosen larger than the size of the unit-cell. This nonlinear filter-

ing is comparable to an automatic gain control. It provides an efficient compensation of slowly varying background nonuniformities (such as gradients across images) and changes in the dynamic range. When working with real images, the use of such an algorithm turned out to be essential: By improving the homogeneity of the data, it largely facilitated the location of control points and produced unit cells with normalized (and almost identical) first-order statistics.

3.2. Selection of reference points

The estimation of the spatial unwarping function requires a set of reference points to be defined (typically, one per unit cell). The technique that has been used to locate these points is based on a standard cross-correlation detection technique. A reference template is either constructed from a characteristic feature that is present in each cell (such as a blob or a line) or from a representative unit cell that has been extracted previously. Note that the first solution when it is applicable is generally preferable because it is less sensitive to spatial deformation. To allow for changes in angular orientation, the reference template may be rotationally symmetrized. The cross-correlation is then computed, by multiplication in the Fourier domain, and the local maxima of this function are searched in real space. The final extraction of a set of reference points is done interactively from a subset of these maxima.

3.3. Unwarping

The estimation of the unwarping function is based on a list of $K \times L$ control points and is described in Section 2. For practical convenience, the gray level values on the new sampling grid are computed from a bilinear interpolation. Note that this technique uses the four closest neighboring pixels and locally approximates the image by a four coefficient bidimensional polynomial function which is computed from an equation similar to (5) or (6).

3.4. Noise reduction

In an unwarped coordinate system, the texture to be analysed may be represented by the superposition of an ideal periodic (signal) and a random component (noise):

$$u_{k,l} = s_{k,l} + n_{k,l}. \tag{10}$$

By construction, the horizontal and vertical periods, T and T', are known integers. By definition, the signal component satisfies:

$$s_{k,l} = s_{k+mT,l+nT'} \tag{11}$$

for any k, l, m, and n. Using this property, both components are separated using a periodicity extracting filter

$$s_{k,l} = \frac{1}{MN} \sum_{m=-M/2}^{M/2} \sum_{n=-N/2}^{N/2} u_{k-mT,l-nT'}. \tag{12}$$

The corresponding frequency response has peaks at multiples of $1/T$ and $1/T'$ in the two principal directions of the spectrum, respectively. The selectivity or noise reduction ability of this filter depends on the number of periods ($M \times N$) that are combined by summation. It can be implemented by successive filtering along the rows and columns. A complete removal of the nonperiodic component is obtained for $M \geq K$ and $N \geq L$. In this particular case, the procedure is equivalent to summing up all available unit cells.

Note that the most desirable feature of unwarping is to maximize the amount of signal or, equivalently, to minimize the amount of noise which is defined as the nonperiodic component. Therefore, the energy of the unwarped periodic signal or, alternatively, the signal-to-noise ratio between both components of model defined by (10), can be used to assess the effectiveness of the whole procedure.

4. Experimental results

This restoration technique has been applied to the analysis of high resolution micrographs

showing the lattice structure of the 'thick', myosin-containing filaments and the 'thin', actin-containing filaments in skeletal muscle [8, 9]. These images were obtained from cryo-sections of specimens preserved by rapid freezing in vitreous ice [5]. This recently developed technique enables the visualization of structural configurations under 'native' conditions, unaffected by artifacts of chemical fixation, dehydration, and staining, as in the conventional thin sectioning methods. The quality of these images can be significantly improved through image processing, which allows for an efficient compensation of the disorders of myofilaments that are exacerbated by compression and deformation imposed in the sectioning process.

4.1. Model experiment

A model representation of relaxed muscle based on X-ray diffraction data [12, 13], was used to generate a periodic structure. This structure was distorted geometrically and corrupted with additive Gaussian noise at a signal-to-noise ratio of one, producing the image shown in Fig. 3(a). In this particular case, because of the uniformity of the data, no preprocessing was necessary and a set of reference points (centered around the myosin thick filaments) were located from the cross-correlation between the warped image in Fig. 3(a) and a rotationally symmetrized reference unit cell. A set of 4×4 reference points was thus extracted and was used to estimate the polynomial coefficients of

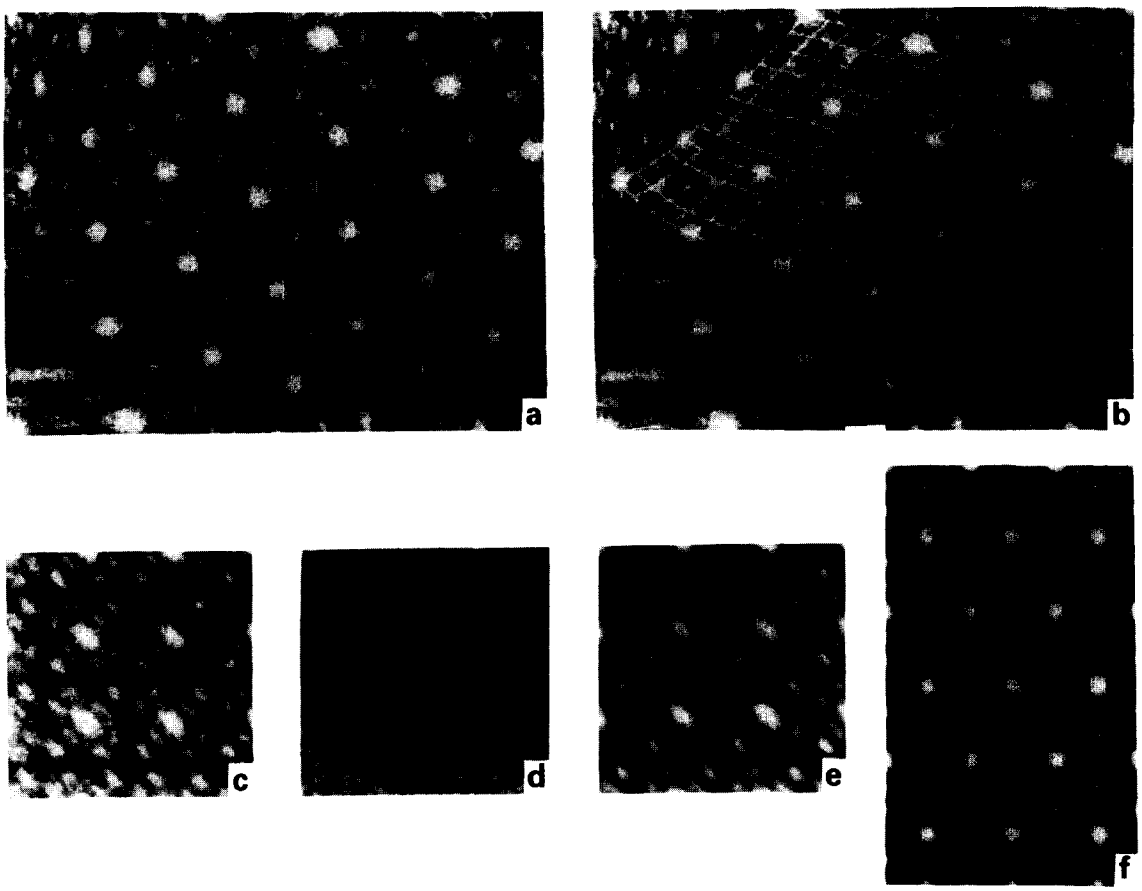

Fig. 3. Example of processing. (a) Distorted model of muscle filaments with additive Gaussian noise with SNR = 1. (b) With superimposed new sampling grid. (c) Unwarped unit cells with 40×40 pixels per cell. (d) Stochastic component. (e) Periodic component. (f) Periodic component displayed in an hexagonal lattice with fully adjusted dynamic range.

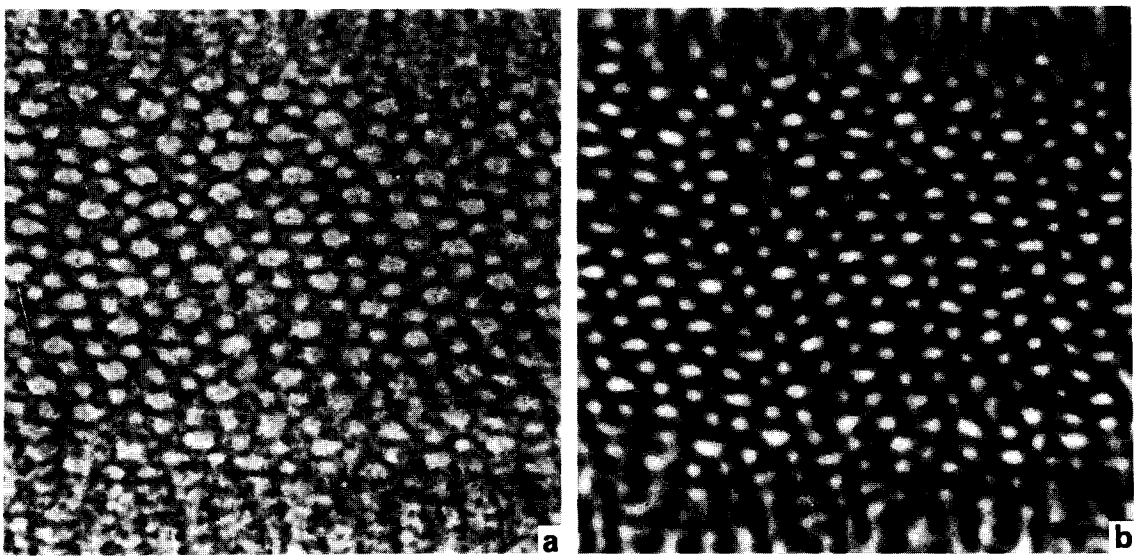

Fig. 4. Myofilament lattice of vertebrate skeletal muscle. (a) 256×256 preprocessed micrograph obtained with a normalization window 55×55. (b) Cross-correlation function computed using a radial filter with a cutoff frequency between 1/12.5 and 1/10 nm^{-1}.

the warping functions according to (5) and (6). The new sampling grid obtained in applying (8) has been superimposed on Fig. 3(b). The result of unwarping with 40×40 pixels per unit cell is displayed in Fig. 3(c). This image was further decomposed in its stochastic and periodic components as shown in Fig. 3(d), (e), respectively. As the unwarping function was designed to map an originally hexagonal unit cell into an ideal square lattice, the extracted periodic component was reconverted into an hexagonal lattice and is displayed in Fig. 3(f) as the final rescaled result of processing. The estimated signal-to-noise ratio obtained in comparing the original structure and the results of this processing is close to 3 and demonstrates the efficiency of this restoration procedure.

4.2. *Analysis of muscle fibers*

A preprocessed portion of an original micrograph showing a transverse cryosection of an overlap region of the myofilament lattice is displayed in Fig. 4(a). This image was obtained on a Philips EM400 electron microscope at a magnification of 15200×, using low-dose techniques, and scanned with a Perkin-Elmer 1010MG to give an effective sampling step of 1.25 nm. A rescaled and rotationally symmetrized version of the central peak, representing the myosin filament in the model unit cell described in the previous section, was used as a reference template. This mask was cross-correlated with the preprocessed micrographs and a maxima searching algorithm was used to locate the control points centered on the 'thick' filaments. This procedure is equivalent to filtering the data with a radially symmetric low-pass filter which acts as a 'blob' detector. As may be visualized on the cross-correlation function displayed in Fig. 4(b), the positions of the 'thick' and 'thin' filaments are identified by characteristic peaks. The discrimination between both types of filaments is based on the size of the peaks as well as on contextual information.

The portion of the image to be analysed was specified interactively by the operator from a subset of 6×5 maxima which satisfied the mapping constraint expressed in Section 2.2. These points were used to estimate the polynomial coefficients of the warping function and to compute the new sampling grid which has been superimposed on Fig. 5(a). The results of the unwarping and noise

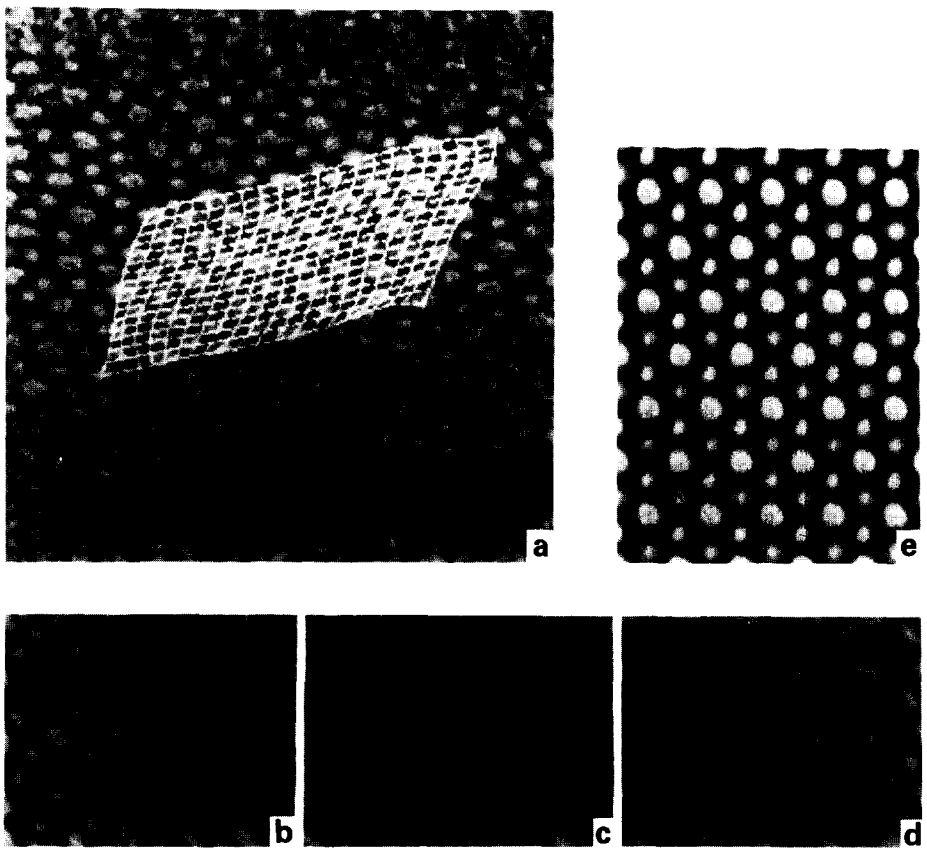

Fig. 5. Example of processing of muscle fibers. (a) Preprocessed micrograph with superimposed sampling grid. (b) Unwarped unit cells with 28×28 pixels per cell. (c) Stochastic component with $\sigma_n^2 = 418.7$. (d) Periodic component with $\sigma_s^2 = 440.6$. (e) Periodic component displayed in an hexagonal lattice with fully adjusted dynamic range.

reduction algorithms are displayed in Fig. 5(b)-(d). The energies of the periodic and stochastic components were 440.6 and 418.7, respectively, corresponding to an estimated signal-to-noise ratio of 1.03. Finally, the averaged square unit cell was mapped into an hexagonal cell producing the rescaled image in Fig. 5(e), which represents a considerable improvement over the original data.

4.3. Discussion

The approach presented here offers a practical system for correcting warped images. Such uncorrected images would be unsuitable for standard correlation averaging (CA) techniques [3, 6]. Correction by CA is limited to translational and rotational alignment and would result in a loss of resolution for warped images. In contrast, preprocessing by an unwarping algorithm before averaging will permit significant improvement of signal-to-noise ratio while maintaining the highest possible resolution.

While the technique presented here has been applied to myofilament thin sections, there are obvious potentialities for the restoration of any deformed lattice structure. In general, the method assures that the extracted unit cells are continuous. The polynomial model of spatial distortion presupposes that the lattice has been deformed in an extremely smooth and continuous fashion. In particular, these assumptions seem appropriate when spatial deformations are due to expansion, com-

pression, or bending of a uniform structure. In addition, the method is suitable for the correction of projection views which may result from nonperpendicular sectioning as well as other applications.

There are a few practical considerations in the utilization of this system. The use of an unwarping algorithm based on bidimensional polynomials should be limited to a maximum of 8×8 unit cells. This results from finite arithmetic precision which can produce nonnegligible roundoff errors in the evaluation of the polynomial coefficients. In addition, higher-order polynomials may have an oscillatory behavior that could introduce noticeable distortions for border unit cells. These potential errors can be minimized when processing large areas by dividing the areas into smaller rectangular patches which may be treated separately, and combined later for noise reduction.

The simplest approach is to use the $4 (= 2 \times 2)$ border points of a single unit cell and to unwarp each cell separately using bilinear polynomials. In such a case, the new sampling grid is piecewise linear with equally spaced sampling steps along these lines. When this simple technique is combined with an algorithm that screens for anomalous images, based on a statistical criterion of consistency [11], satisfactory preliminary results have been obtained [8, 9]. This approach may also be useful when the image contains cells of nonuniform structural material, and which may not be continuous at the unit cell reference points (for example, irregular tetragons).

The methodology described by the block diagram in Fig. 2 is not restricted to the use of polynomial representations only. It may easily be adapted for other models of spatial deformation. An alternative approach, which is currently under investigation, uses bi-cubic spline functions.

5. Conclusion

A method that compensates for spatial distortions of quasi-periodic structures has been presented. This approach geometrically transforms the data by mapping of a warped or skewed lattice into an ideal rectangular lattice based on a set of previously detected reference or control points. Following this transformation, standard noise reduction techniques such as cumulative averaging or periodic filtering can be applied. This procedure enables a significant improvement of high resolution micrographs of crystalline or quasi-periodic structures such as found in muscle fibers, and should therefore provide a useful tool for the structural investigation of organized biological systems.

The most sensitive step of processing is the selection of control points which is presently supervised by the experimentator. We shall continue research for the improvement of this procedure and study the possibility of an iterative system where the currently determined structure is used to refine the detection of the reference points.

Acknowledgment

We thank Dr. A.C. Steven for helpful discussions on algorithm design, and Drs. R.J. Podolsky, A.C. Steven, A.W. McDowall, and J. Dubochet for making available the electron micrographs. We are grateful to Dr. L.C. Yu for a digital model of the myofilament lattice.

References

[1] J.L. Carrascosa and A.C. Steven, "A procedure for evaluation of significant structural differences between related arrays of protein molecules", *Micron*, Vol. 9, 1979, pp. 199-206.

[2] M. Eden, M. Unser and R. Leonardi, "Polynomial representation of pictures", *Signal Processing*, Vol. 10, No. 4, June 1986, pp. 385-393.

[3] J. Frank, A. Verschoor and M. Boublik, "Computer averaging of electron micrographs of 40S ribosomal subunits", *Science*, Vol. 214, 1981, pp. 1353-1355.

[4] U. Grenander, *Pattern Synthesis, Lectures of Pattern Theory, Vol. I*, Springer, Berlin, 1976.

[5] A.W. McDowall, W. Hofmann, J. Lepault, M. Adrian and J. Dubochet, "Cryo-electron microscopy of vitrified insect flight muscle", *J. Mol. Biol.*, Vol. 178, 1984, pp. 105-111.

[6] W.O. Saxton, *Computer Techniques for Image Processing in Electron Microscopy*, Academic Press, New York, 1978.

[7] P.R. Smith and U. Aebi, "The computer filtration of hexagonal lattices", *J. Supramolec. Structure*, Vol. 5, 1976, pp. 493-495.

[8] A.C. Steven, B.L. Trus, M. Unser, A.W. McDowall, J. Dubochet and R.J. Podolsky, "Myofilament lattice of vertebrate skeletal muscle visualized by correlation averaging of frozen hydrated thin sections", in G.W. Bailey, ed., *Proc. 44th Ann. Meeting of the Electron Microscopy Society of America*, San Francisco Press, August 1986, pp. 108-109.

[9] B.L. Trus, A.C. Steven, M. Unser, A.W. McDowall, J. Dubochet and R.J. Podolsky, "Correlation averaging techniques to rectify disordered myofilament lattices visualized in frozen hydrated thin sections of vertebrate muscle", *Proc. XIth Internat. Congress on Electron Microscopy*, August 31-September 7, Kyoto, Japan, 1986, 3103-3104.

[10] M. Unser, "Description statistique des propriétés de textures: Application à l'inspection automatique", Thèse de Doctorat Es Sciences Techniques No. 534, Laboratoire de Traitement des Signaux, École Polytechnique Fédérale de Lausanne, Switzerland, 1984.

[11] M. Unser, A.C. Steven and B.L. Trus, "Odd Men Out: A quantitative objective procedure for identifying anomalous members of a set of noisy images of ostensibly identical specimens", *Ultramicroscopy*, Vol. 19, 1986, pp. 337-348.

[12] L.C. Yu and B. Brenner, "High-resolution equitorial X-ray diffraction from single rabbit Psoas fibers", *Biophys. J.*, Vol. 49, 1986, pp. 133-135.

[13] L.C. Yu, A.C. Steven, G.R.S. Naylor, R.C. Gamble and R.J. Podolsky, "Distribution of mass in relaxed frog skeletal muscle and its redistribution upon activation", *Biophysical J.*, Vol. 47, 1985, pp. 311-321.